Journal of NeuroVirology, 15: 57–70, 2009

ISSN 1355-0284 print / 1538-2443 online
DOI: 10.1080/13550280802482583

informa
healthcare

Neurons and oligodendrocytes in the mouse brain differ in their ability to replicate Semliki Forest virus

Rennos Fragkoudis,[1] Nele Tamberg,[2] Ricky Siu,[1] Kaja Kiiver,[2] Alain Kohl,[1] Andres Merits,[2] and John K. Fazakerley[1]

[1]*The Roslin Institute and Royal School of Veterinary Studies, College of Medicine and Veterinary Medicine, University of Edinburgh, UK; and* [2]*Institute of Technology, University of Tartu, Estonia*

Semliki Forest virus (SFV) provides an experimental model of acute virus encephalitis and virus-induced demyelinating disease. Two marker viruses expressing fluorescent proteins as part of the replicase or the structural open reading frame were used to evaluate virus replication in cells of the adult mouse brain. Both marker viruses established a high-titer infection in the adult mouse brain. As determined by location, morphology, and immunostaining with neural cell type–specific phenotypic markers, both viruses infected neurons and oligodendrocytes but not astrocytes. Determination of eGFP expression from either the replicase or the structural open-reading frame coupled with immunostaining for either the virus structural protein or the virus nonstructural protein-3 readily distinguished cells at early and late stages of infection. Neurons but not oligodendrocytes rapidly down-regulated virus replication. Rapid down-regulation of virus replication was also observed in mature but not immature primary cultures of rat hippocampal neurons. This study demonstrates for the first time that *in vivo* central nervous system (CNS) cells differ in their ability to suppress alphavirus replication. *Journal of NeuroVirology* (2009) **15,** 57–70.

Keywords: alphavirus; Semliki Forest virus; neuron; oligodendrocyte

Introduction

Arboviruses, particularly in the virus families *Togaviridae, Flaviviridae,* and *Bunyaviridae,* are major causes of viral encephalitis. These viruses are spread to vertebrates by arthropod vectors, primarily mosquitoes and ticks. Important examples include Venezuelan equine, Japanese, West Nile, and California encephalitis viruses. Alphavirus (family *Togaviridae*) infections of rodents have been extensively studied as models of virus encephalitis. Alphaviruses have a positive-strand RNA genome of approximately 12 kb, which contains two open-reading frames encoding the nonstructural, or replicase, and the structural polyproteins (Strauss and Strauss, 1994). The pathogenesis of alphavirus encephalitis depends upon virus and host genetics, which determine the central nervous system (CNS) cell types infected, restricted or productive infection, and whether infected cells and animals die, clear the infection, or become persistently infected (Atkins *et al*, 1999; Fazakerley, 2002; Griffin, 2005).

In the mouse, all strains of the encephalitic alphavirus Semliki Forest virus (SFV) that have been studied to date infect both neurons and oligodendrocytes (Pathak and Webb, 1983; Gates et al, 1985; Fazakerley et al, 2006). All strains of SFV replicate efficiently in immature cells of the developing mouse brain and infection of neurons is productive and results in apoptotic death, panencephalitis, and rapid death of the animal (Oliver et al, 1997; Allsopp and Fazakerley, 2000). In contrast, the course of CNS infection in the adult mouse depends on virus strain and ranges from fulminant encephalitis with the L10 strain to a

The authors are grateful to Dr. Eva Zusinaite for her help with the biochemical analyses. This work was funded by the EU SFVECTORS (www.sfvectors.ed.ac.uk) programme.

Address correspondence to John K. Fazakerley, Virology, Centre for Infectious Diseases, College of Medicine & Vet Medicine, University of Edinburgh, Summerhall, Edinburgh EH9 1QH, UK. E-mail: John.Fazakerley@ed.ac.uk

Received 30 April 2008; revised 16 July 2008; accepted 3 September 2008

subclinical demyelinating encephalomyelitis with the A7(74) strain (Pusztai et al, 1971; Fazakerley et al, 1993). The SFV4 strain is generated by *in vitro* transcription and transfection of RNA from an infectious cDNA clone (pSFV4) derived from the virulent prototype strain (Liljestrom et al, 1991). SFV4 is neurovirulent; adult mice rapidly die of a fulminant encephalitis following intracerebral inoculation (Fazakerley et al, 2002). However, following intraperitoneal or intranasal inoculation of adult mice, SFV4 is only virulent at very high doses (Glasgow et al, 1991; Tarbatt et al, 1997; Tuittila and Hinkkanen, 2003). Low doses fail to establish a high-titer viremia and virus does not enter the CNS (Fragkoudis et al, 2007). The A7(74) strain is efficiently neuroinvasive even when inoculated at low doses, but infection of neurons in the adult mouse brain is restricted (Fazakerley et al, 1993). Restricted replication in neurons is not dependent upon the type I interferon system but intriguingly can be alleviated by treating mice with gold compounds (Scallan and Fazakerley, 1999; Fragkoudis et al, 2007). If SFV A7(74) virus is inoculated directly intracerebrally, at least at early time points, in contrast to the restricted replication in neurons, oligodendrocytes appear to be permissive for productive virus replication and virus spreads in white matter tracts (Fazakerley, 2002; Fazakerley *et al*, 2006). Restriction of virus replication in mature neurons is also observed with other viruses, including lymphocytic choriomeningitis virus and measles virus (Oldstone and Buchmeier, 1982; Liebert et al, 1986, 1990). Given that restricted infection may be related to the differentiation state of the cell, studying this phenomenon is particularly difficult as cells of neuronal or oligodendroglial origin in continuous culture *in vitro* may not be reliable models of events in postmitotic cells *in vivo*.

We have previously described the construction and characterization of SFV4(3H)-eGFP in which eGFP is cloned into the SFV4 replicase open-reading frame between nonstructural protein (nsP)-3 and -4. Processing of the translated polyprotein releases free eGFP with a very short half-life (Tamberg *et al*, 2007). In this study, in order to monitor expression of the structural open-reading frame, we have constructed and characterized a second recombinant virus with eGFP cloned between the capsid protein and the glycoproteins of the structural open-reading frame of SFV4. We have then used these two marker viruses to study virus replication directly *in vivo* in cells of the adult mouse brain. As expected from previous studies, both viruses infected neurons and oligodendrocytes but virus replication differed in these two cell types; neurons but not oligodendrocytes rapidly shut down expression of the virus replicase, demonstrating that these two cell types have a different course of virus infection.

Results

Construction and characterization of a recombinant SFV expressing eGFP from the virus structural open-reading frame

We have previously described construction and *in vitro* characterization of SFV4(3H)-eGFP (Figure 1a), this correctly processes the replicase polyprotein and releases eGFP, which has a very short (<2 h) half-life (Tamberg *et al*, 2007). This short half-life is useful for virus infection studies because fluorescence intensity closely reports protein synthesis. To generate a virus expressing eGFP from the structural open-reading frame (ORF), eGFP was cloned into the SFV4 structural ORF between the capsid and E2 sequences (Figure 1b). This new icDNA was designated pSFV4-steGFP. SFV4-steGFP, SFV4(3H)-eGFP, and SFV4 were generated from their respective icDNAs by electroporation of *in vitro* transcribed RNAs into BHK-21 cells. Immunoblotting studies on lysates from BHK-21 cells infected with these viruses (Figure 1c) demonstrated that the structural polyprotein of the newly constructed SFV4-steGFP was processed to release both free capsid and free eGFP. Low levels of a series of high-molecular-mass proteins containing eGFP, most notable one corresponding to an eGFP-2A-p62 fusion protein, were also apparent. In contrast to eGFP derived from SFV4(3H)-eGFP, the half-life of eGFP derived from SFV4-steGFP was in excess of 16 h (Figure 1d).

To determine the viability of SFV4-steGFP and compare its replication to SFV4(3H)-eGFP and SFV4, one-step growth curves were carried out in BHK-21 cells (Figure 1e). As with SFV4(3H)-eGFP, SFV4-steGFP replicated less well than SFV4, titers of both viruses were significantly lower ($P<.05$; paired t test) than SFV4 at all time points; nevertheless both recombinant viruses replicated to high titers, indicating that insertion of eGFP had no major effect on virus viability. In BHK-21 cells infected with SFV4(3H)-eGFP, fluorescent signal was detected as early as 2 h, this increased until 6 h and then rapidly decreased. Late in infection these cells had a dull green fluorescence. In cells infected with SFV4-steGFP, fluorescence, first clearly visible at 5 h, reached its peak between 10 and 12 h and remained high over 48 h. Cells in all three virus-infected cultures were rounded up and dead by 48 h.

To investigate the distribution of eGFP relative to that of virus replication complexes, cells were immunostained to visualize the nsP3 protein. As expected, nsP3 was detected in the cytoplasm of cells infected with SFV4 and both marker viruses. nsP3 staining was always punctate and predominantly perinuclear, a staining pattern consistent with the known distribution of virus replication complexes on cytopathic vacuoles (Lemm and Rice, 1993; Kujala et al, 2001; Salonen et al, 2003). The

distribution of eGFP differed between the two marker viruses (Figure 2a and b). In SFV4(3H)-eGFP infected cells, fluorescence was observed throughout the cytoplasm and the nucleus and was most intense in the nucleus. The absence of colocalization between eGFP and nsP3 indicated that eGFP was cleaved efficiently from the replicase polyprotein. Immunostaining for virus structural proteins (data not shown) demonstrated many double-labeled cells but some eGFP-positive cells were immunostain-negative; these were presumably cells at the early stage of infection. In SFV4-steGFP–infected cells, eGFP fluorescence was predominantly cytoplasmic and perinuclear but clearly separate from nsP3. Cells at early (nsP3-positive/eGFP-negative) and late (nsP3-positive/eGFP-positive) stages of infection were evident. Immunostaining for virus capsid or envelope glycoproteins (data not shown) demonstrated, as expected, immunostaining of all eGFP-positive cells.

To determine if the eGFP marker viruses remained competent to infect and express eGFP in mosquito cells, continuous cultures of C6/36 mosquito cells (*Aedes albopictus)* were infected with the marker viruses. In C6/36 cells, as in BHK-21 cells, infection with SFV4(3H)-eGFP resulted in both cytoplasmic and nuclear eGFP expression and punctate cytoplasmic nsP3 staining (Figure 2c). In C6/36 cells infected with SFV4-steGFP, eGFP was expressed to high levels but in contrast to BHK-21 cells, eGFP was distributed throughout the cytoplasm and nucleus; some of the nuclei were brighter than the surrounding cytoplasm (Figure 2d). Again nsP3-specific staining of these cells showed the characteristic punctate cytoplasmic pattern observed previously. Over 5 days of study, no cytopathic

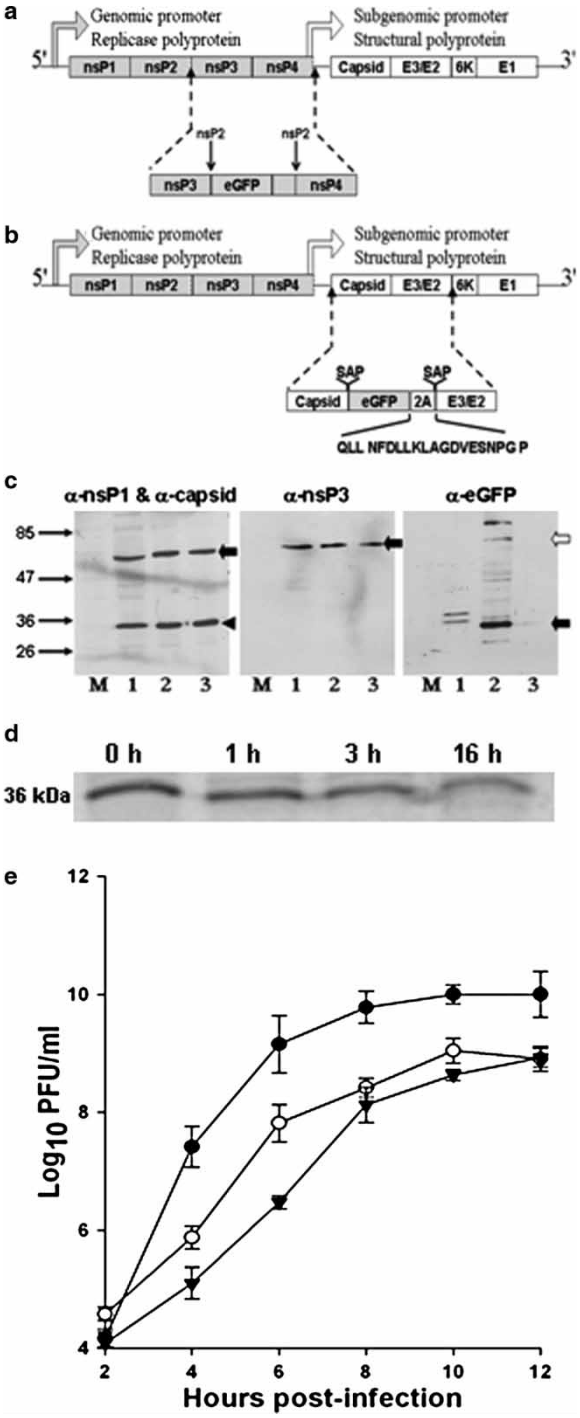

Figure 1

Figure 1 (**a**) Schematic representation of the construction of SFV4(3H)-eGFP. The coding sequence for eGFP was flanked by nsP2 protease-recognition sites (↓) and inserted between nsP3 and nsP4; Tamberg *et al* (2007). (**b**) Schematic representation of SFV4-steGFP; eGFP was inserted between the capsid protein and p62 (E2/3). The first three amino acids of p62 (SAP) were inserted after the capsid and 2A to ensure correct processing. The FMDV 2A sequence and the preceding three amino acids from the FMDV 1D protein and the following proline from the FMDV 2B sequence are shown in full. (**c**) Western blotting on cell lysates of BHK-21 cells infected for 6 hours with SFV4(3H)-eGFP (1), SFV4-steGFP (2), or SFV4 (3) (MOI 20) or mock-infected (M; PBSA) and immunostained as indicated above each panel. Specific bands of the appropriate molecular weight for nsP1, nsP3, and eGFP are indicated with solid arrows. The eGFP size difference (~2 kDa) between SFV4(3H)-eGFP and SFV4-steGFP results from different processing of the nonstructural and structural ORF which respectively adds 37 and 22 amino acids to eGFP. The nature of the upper eGFP band in lane 1 is not clear and is not always apparent (Tamberg *et al*, 2007). The band corresponding to capsid is indicated by an arrowhead. The open arrow highlights a band with the size of an eGFP-2A-p62 fusion protein. (**d**) Stability of eGFP; replicate cultures of BHK21 cells were infected with SFV4-steGFP (MOI 10). Six hours post infection, cells were pulsed with ^{35}S-Met/Cys. Cells were lysed after 45 min pulse (0) or after chase for 1, 3, or 16 h and immunoprecipitated eGFP was run on an SDS-gel. (**e**) Monolayers of BHK-21 cells were infected in triplicate with SFV4 (●), SFV4(3H)-eGFP (○), or SFV4-steGFP (▼) at an MOI of 10 to compare growth kinetics. Each point represents the mean of three samples; the bars represent the standard deviation. Values at each time point were compared using paired *t* test. At all time-points, recombinant viruses had significantly ($P < .05$) lower titers than SFV4.

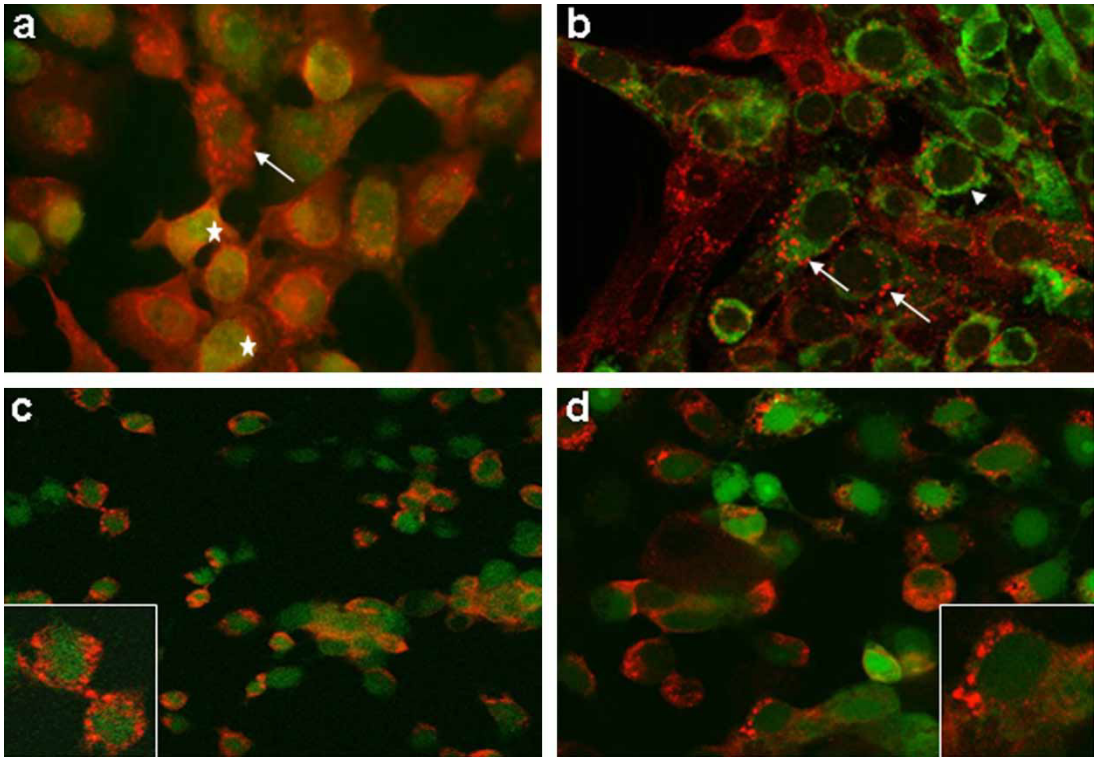

Figure 2 BHK-21 cells infected (MOI 10) with SFV4(3H)-eGFP for 6 h (**a**) or with SFV4-steGFP for 12 h (**b**) and immunostained for nsP3 (*red*) had a punctate cytoplasmic distribution (*arrows*) of nsP3. In SFV4(3H)-eGFP–infected cells, eGFP was observed in both cytoplasm and nucleus (*). In SFV4-steGFP infected cells, fluorescence was predominantly cytoplasmic and perinuclear (*arrowhead*). C6/36 cells infected (MOI 10, 16 h) with SFV4(3H)-eGFP (**c**) or SFV4-steGFP (**d**) had both cytoplasmic and nuclear eGFP; high power images are shown in the insets. This figure is reproduced in colour in *Journal of Neurovirology* online.

effect was observed in C6/36 cells infected with SFV4, SFV(3H)-eGFP or SFV4(3H)eGFP.

Genetic stability in BHK-21 cells and mice

To determine the genetic stability of the marker viruses, each virus was passaged five times through BHK-21 cells at a multiplicity of infection (MOI) of 0.01 or five times through adult mouse brains. After each passage, 96 plaques were transferred to monolayers of BHK-21 cells on 96-well plates and screened for eGFP expression. RNA was also isolated from an aliquot of each cell passage and assessed by polymerase chain reaction (PCR) amplification using primers spanning the site of eGFP insertion (data not shown). Table 1 shows the phenotypic stability of the two viruses. Upon passage in BHK-21 cells, SFV4(3H)-eGFP was considerably more stable than SFV4-steGFP but both viruses showed good stability upon *in vivo* passage through mouse brains.

Course of infection in adult mice

In adult mice, irrespective of the route of inoculation, the two most studied SFV strains, SFV L10 and SFV A7(74), are virulent and avirulent, respectively. In adult mice, SFV4 is virulent if given at high dose intranasally or intracerebrally but is avirulent when inoculated intraperitoneally, at least at 5000 plaque-forming units (PFU) (Glasgow et al, 1991; Fragkoudis et al, 2007). To assess the virulence of the eGFP marker viruses, groups ($n = 6$) of adult (4- to 5-week-old, female) Balb/c mice were inoculated intraperitoneally with 5000 PFU of SFV4, SFV4(3H)-eGFP, SFV4-steGFP, SFV L10, or SFV A7(74) or mock-infected with PBSA (PBS containing 0.75% of bovine serum albumin [BSA]). Mice infected with SFV L10 were dead or had reached clinically

Table 1 Phenotypic stability of SFV4(3H)-eGFP and SFV4-steGFP after each of five passages (P1 to P5) through BHK-21 cell cultures (*in vitro)* or through adult mouse brain (*in vivo*)

	P1	P2	P3	P4	P5
In vitro					
SFV4(3H)-eGFP	100%	100%	98.9%	95.2%	93.6%
SFV4-steGFP	100%	96.9%	78.6%	2%	0%
In vivo					
SFV4(3H)-eGFP	100%	100%	100%	100%	98.9%
SFV4-steGFP	100%	100%	100%	100%	94.8%

Note. After each passage, culture supernatant or brain homogenate was plaqued on BHK-21 cells and eGFP fluorescence of 96 plaques was assessed by transfer of each onto a monolayer of BHK-21 cells in a 24-well plate. The indicator monolayers were observed by fluorescence microscopy. The percentage of plaques giving rise to eGFP-positive monolayers is shown.

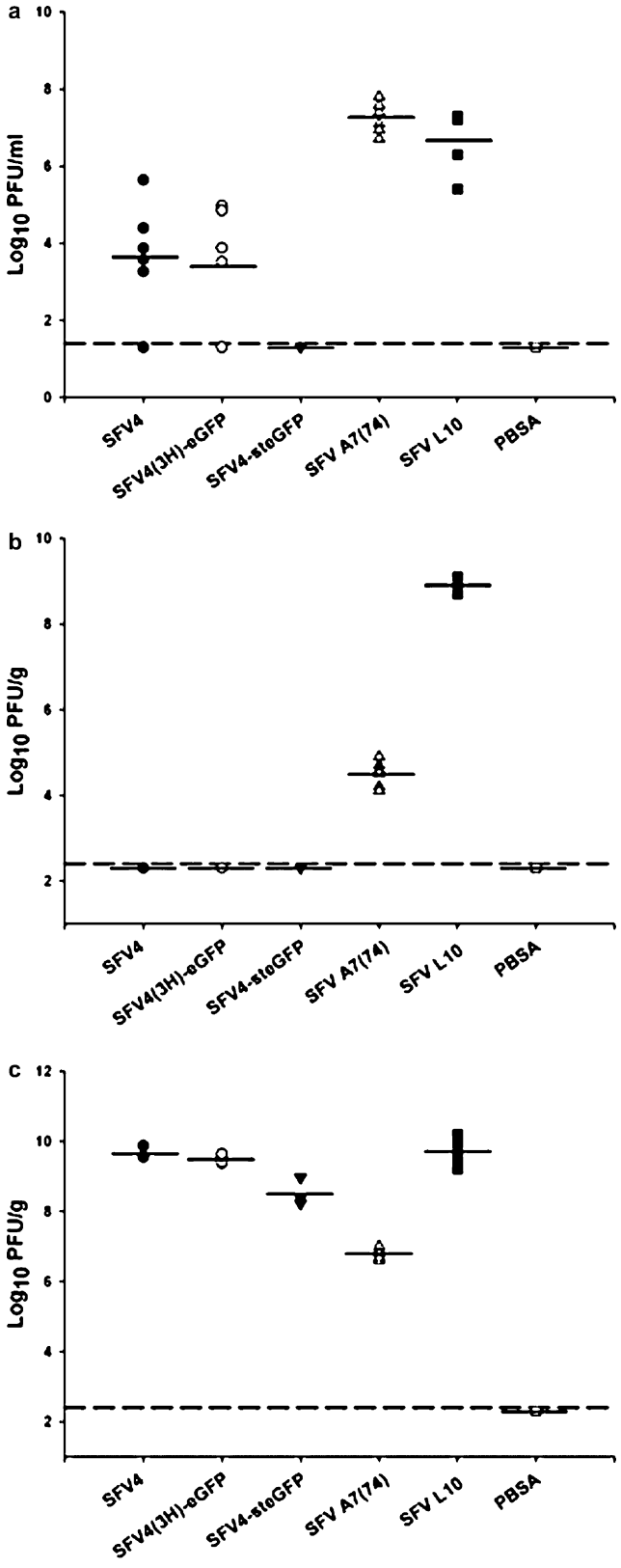

Figure 3

defined terminal end points, indicative of fatal encephalitis by day 3. Mice infected with the other viruses were monitored for 2 weeks and remained healthy with no clinical signs of infection. A repeat experiment using 100-fold more virus produced the same result.

To compare virus replication in adult mice, groups of mice were inoculated intraperitoneally with 5000 PFU of SFV4, SFV4(3H)-eGFP, SFV4-steGFP, SFV L10, or SFV A7(74) or mock-infected with PBSA and mice were sampled at each of days 1 and 4, or days 1 and 3 for the more virulent SFV L10. Day 1 blood and day 4 or 3 half brains were titrated for virus and the other half brains were screened by fluorescent microscopy for eGFP-positive cells. In the blood at 24 h, virus was detectable in all mice in all groups except for mock-infected mice and mice infected with SFV4-steGFP (Figure 3a). There was no significant difference (paired *t* test) in blood virus titer between SFV4 and SFV4(3H)-eGFP ($P > .05$), but titers of both these viruses were significantly lower than those of both SFV L10 and SFV A7(74) ($P < .05$). The results indicate that relative to SFV4, in adult mice, extraneural replication of SFV4(3H)-eGFP was not attenuated but extraneural replication of SFV4-steGFP was strongly attenuated. It is also apparent that SFV4 and viruses derived from it replicate less efficiently, at least outside the CNS, than SFV A7(74) or SFV L10; this is consistent with our previous results (Fragkoudis *et al*, 2007).

High titers of infectious virus were present in the half brains taken for virus titration from mice infected with SFV L10 or SFV A7(74) but no infectious virus was detectable in the brains of mice infected with SFV4, SFV(3H)-eGFP, or SFV4-steGFP (Figure 3b). Examination of frozen brain sections (>18 sections per brain) from the other half brains of the mice infected with SFV(3H)-eGFP or SFV4-steGFP showed no eGFP expression at day 4. Together, these results indicate that following intraperitoneal inoculation, SFV4-based viruses did not cross the blood-brain barrier or at least had not done so by 4 days post infection, or alternatively that they had the capacity to cross the blood-brain barrier but not to replicate in the brain.

To determine whether the recombinant eGFP marker viruses were capable of replicating in the brain, groups of mice were infected intracerebrally with 1000 PFU of the different viruses or mock-infected

Figure 3 Groups ($n = 12$) of 4- to 5-week-old, female, Balb/c mice were infected (5000 PFU) intraperitoneally with SFV4 (●), SFV4(3H)-eGFP (○), SFV4-steGFP (▼), SFV A7(74) (△), SFV L10 (■) or were mock-infected with PBSA (□) and sampled ($n = 6$) at 24 h or at 4 days (3 days for SFV L10). Virus titers in the blood at 24 h (**a**) and the brain at 3 or 4 days (**b**). (**c**) Groups ($n = 6$) of 4- to 5-week-old, female, Balb/c mice were infected (1000 PFU) intracerebrally with the same viruses and sampled upon reaching clinically defined terminal end points. In all panels, each point represents a single mouse; the horizontal lines indicate the means, the dashed lines indicate the limit of detection. Titers were determined by standard plaque assay.

with PBSA. All animals infected with SFV L10, SFV4, and SFV4(3H)-eGFP reached clinically defined terminal end points, indicative of substantial disease by 48 h, and were killed and the brains sampled. The course of infection in SFV4-steGFP–infected mice was slower, but all mice reached clinically defined terminal end points by 72 h. The SFV A7(74)–infected mice showed no clinical signs but were also sampled at 72 h. Half brains were titrated for virus and half were processed for histopathological study. All animals infected with each of the viruses had high levels of infectious virus in the brain (Figure 3c), indicating that these SFV4-based viruses were not attenuated in their ability to replicate and spread in the adult mouse brain. SFV4 and SFV4(3H)-eGFP reached statistically significantly higher titers than SFV4-steGFP ($P < .05$). It can be concluded that *in vivo* in the mouse brain, SFV4-steGFP was slightly attenuated relative to SFV4.

eGFP expression and virus tropism in the adult mouse brain

Histopathological study of brains infected with SFV4(3H)-eGFP demonstrated few eGFP-positive cells. Positive cells, which were generally dull green, were most frequently observed in white matter tracts (Figure 4a and b). Immunostaining for nsP3 demonstrated, as expected, that all eGFP-positive cells were nsP3-positive. As with cells in culture, nsP3 immunostaining was punctate and cytoplasmic. Except in white matter tracts, nsP3-positive eGFP-negative cells greatly out numbered double-labeled cells (Figure 4c and d). Many cells clearly identifiable as neurons by their anatomical location and morphology, for example pyramidal neurons of the hippocampus, and many other cells with a neuronal morphology were nsP3-positive but eGFP-negative (Figure 4c). Dull green, eGFP-positive cells clearly identifiable by location or morphology as neurons were observed but only rarely (Figure 4d). Small double-positive cells were often observed adjacent to larger nsP3-positive cells with a neuronal morphology (Figure 4c and d). The position and morphology of these double-labeled cells was consistent with their being satellite oligodendrocytes. Additional sections were immunostained with an antibody to the virus structural proteins. As with nsP3 staining, this demonstrated large numbers of virus structural protein–positive cells that were eGFP-negative (Figure 4e and f). In contrast to nsP3 staining, only a small proportion (1% to 5%) of the eGFP-positive cells was also positive for structural proteins (Figure 4f). This is consistent with early expression of the nonstructural ORF and late expression of the structural ORF. Taken together, these studies demonstrate that whereas virus replication complexes (nsP3) were long-lived and present in both neurons and oligodendrocytes, eGFP expression indicative of replicase synthesis was observed only at low levels and only rarely in infected neurons but was common in infected oligodendrocytes, suggesting that neurons but not oligodendrocytes rapidly shut down synthesis of replicase proteins. As determined by immunostaining, virus structural proteins were synthesized in both cell types.

In brains infected with SFV4-steGFP, there was extensive eGFP expression with widespread infection of the corpus callosum and other white matter tracts and large foci of eGFP-expressing cells scattered throughout the brain (Figure 4g). There was considerable variation in the level of eGFP expression. Some cells had very bright fluorescence and most cells were brighter than cells infected with SFV4(3H)-eGFP. In contrast to SFV4(3H)-eGFP infection, cells with locations and morphologies consistent with both neurons as well as oligodendrocytes were eGFP-positive. In neurons, eGFP was present throughout the cell body, nucleus and axons (Figure 4g). In putative oligodendrocytes, eGFP fluorescence was concentrated in the cytoplasm (Figure 4h). Immunostaining for nsP3 demonstrated

Figure 4 Distribution of infected cells in the brains following intracerebral inoculation with SFV4(3H) (**a**–**f**) or SFV4-steGFP (**g**–**n**). (**a**) eGFP expression in cells in white matter (wm) tracts (apparent as areas of brighter background staining). The chain-like arrangement of cells (*dashed line*) is characteristic of oligodendrocytes. (**b**) Higher power showing eGFP-positive cells in the white matter (brighter background area lower right). These cells were generally dull green. Occasionally bright green cells (*arrow*) were also observed. (**c**) Section from the dentate gyrus of the hippocampus containing large numbers of neurons showing the extent of infection as determined by nsP3 immunostaining. Most nsP3-positive cells were not eGFP-positive. The arrows and the higher power inset show that many eGFP-positive cells were small and consistent with satellite oligodendrocytes. (**d**) In some areas of infection, double-labeled cells were observed (*arrows*). (**e**) Immunostaining for virus structural protein (*red*) also showed that the majority of infected cells outside white matter tracts did not express eGFP; cells in the white matter (to the right of the dashed line) were generally eGFP-positive. (**f**) Occasional cells in the grey matter were eGFP-positive but had no or low levels of structural protein (*arrowheads*), some of these were perineuronal, consistent with satellite oligodendrocytes (*arrow*), occasional cells were double labeled (*). Many infected cells were eGFP-negative. (**g**) eGFP expression in oligodendrocytes in the white matter of the corpus callosum (cc) and the pyramidal neurons (P) of the hippocampus. In the latter, eGFP is present in the nucleus, cytoplasm, and neurites. (**h**) eGFP expression in oligodendrocytes in a white matter tract. These cells show the characteristic chain-like distribution (*dashed line*) of oligodendrocytes. eGFP was present in both the nucleus and cytoplasm. (**i**) A focus of infection in the cortex showing eGFP and nsP3 staining (*red*); (**j** and **k**) separate red and green channels for the lower half of **i**. Together these panels demonstrate that the cells around the expanding edge of this focus of infection were nsP3-positive but eGFP-negative (*arrowhead*), consistent with recent infection, whereas others (*arrow*) were strongly eGFP-positive but also nsP3-positive consistent with later stages of infection and long-life of the replicase complexes. (**l**) Two foci of infection in the cortex showing eGFP and immunostaining for structural virus proteins (*red*); (**m** and **n**) separate red and green channels for the lower half of **l**. All infected cells were double labeled. The bar in **b, d, f,** and **h** represents 20 μm and in all other panels 100 μm. This figure is reproduced in colour in *Journal of Neurovirology* online.

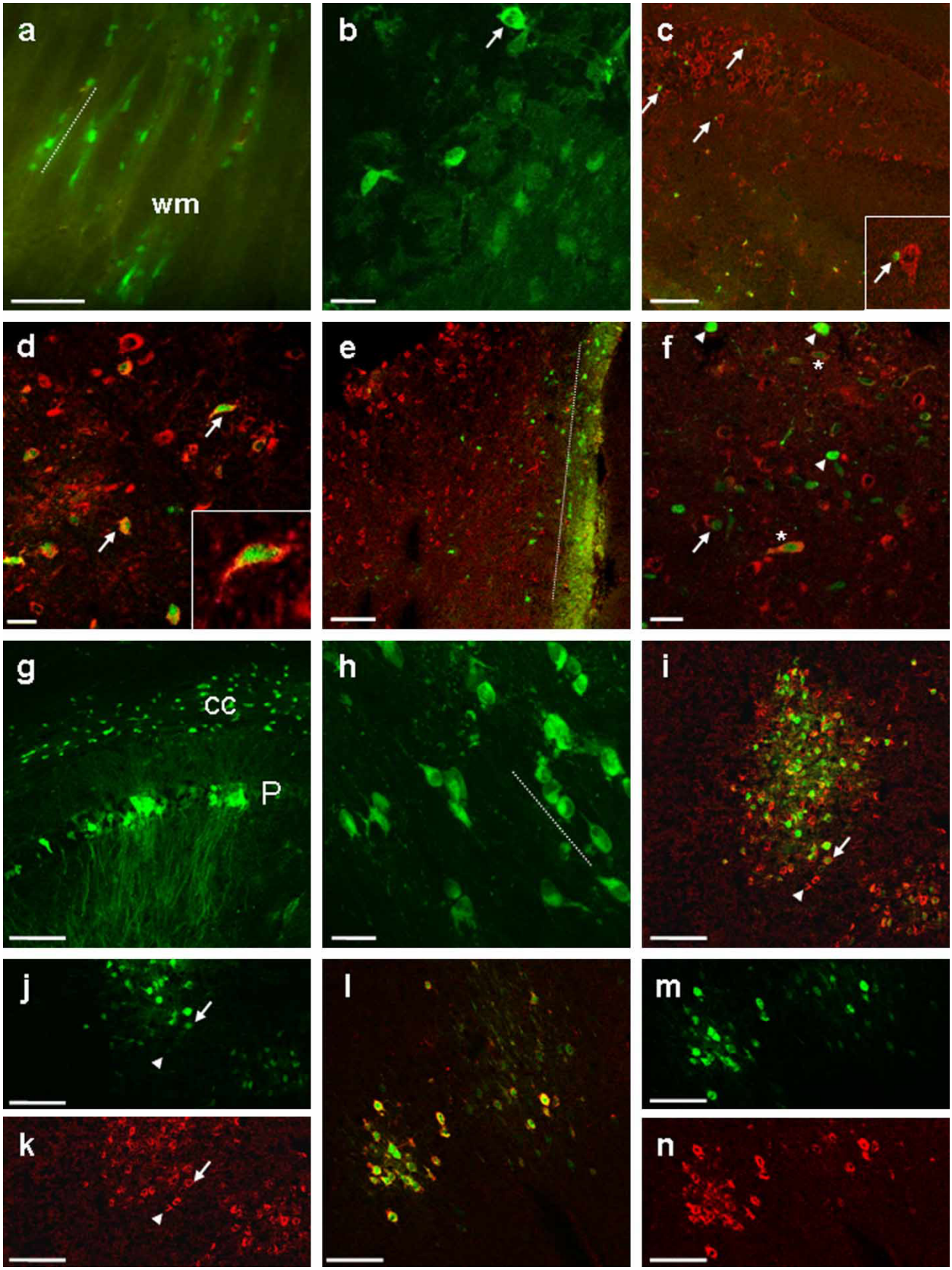

Figure 4 (*Continued*)

that the majority of eGFP-positive cells were also nsP3-positive but nsP3-positive eGFP-negative cells were also observed. The latter were most common around the expanding edge of foci of infection (Figure 4i to k). An inverse relationship was sometimes apparent between the intensity of nsP3-staining and eGFP fluorescence; eGFP-dull cells stained strongly for nsP3 whereas eGFP-bright cells stained weakly for nsP3. This inverse staining and the presence of nsP3-positive eGFP-negative cells around the edge of foci are both consistent with a switch from replicase to structural protein synthesis. Staining for virus structural proteins was coincident with eGFP expression (Figure 4l to n). Rarely, eGFP-positive structural protein–negative cells were observed. These were presumed to be cells that had just started to translate the structural ORF in which eGFP detection was more sensitive than the immunostaining. Taken together, these studies demonstrate that both neurons and oligodendrocytes switch to structural protein synthesis. SFV4-steGFP provides a reliable marker of infected cells, detecting all infected cells except those most recently infected.

To investigate virus tropism in greater detail, sections from brains infected with the eGFP marker viruses were stained with antibodies to brain cell phenotypic markers. Neurons were stained with antibody to the neuron-specific protein NeuN, present in the nuclei and perikarya of most CNS neurons; oligodendrocytes with an antibody to 2′3′-cyclic nucleotide 3′-phosphohydrolase (CNPase) and astrocytes with an antibody against glial fibrillary acidic protein (GFAP). In SFV4(3H)-eGFP–infected brains, many eGFP-positive oligodendrocytes were observed but again eGFP fluorescence was only rarely observed in neurons and never in astrocytes (Figure 5a, c, d, g, and i). In SFV4-steGFP–infected brains, eGFP fluorescence was observed in both oligodendrocytes and neurons but not in astrocytes (Figure 5b, e, f, h, and j). These observations are consistent with those based on cell morphological and anatomical identification of cell phenotypes.

Infection of postmitotic hippocampal neurons in vitro

To investigate whether the rapid shut-off of the virus replicase could be also be observed in neurons *in vitro*, mature (19 days in culture), replicate cultures of postmitotic rat hippocampal neurons were infected with SFV4(3H)eGFP or SFV4-steGFP. Cultures infected with SFV4(3H)eGFP had low levels of eGFP expression at 4 h post infection but were eGFP-negative by 16 h (Figure 6a). In contrast, from around 8 h, rat hippocampal neurons infected with SFV4-steGFP maintained high level eGFP fluorescence that was evenly distributed throughout the cytoplasm, including axonal processes and the nucleus (Figure 6b). To quantitate events, viruses in which eGFP was replaced with *Renilla* luciferase (*RLuc*) were constructed. These viruses, SFV4(3H)-*RLuc* and SFV4-st*RLuc*, were used to infect replicate cultures of immature or mature hippocampal neurons and *RLuc* activity was measured at 4, 8, and 16 h post infection (Figure 7). *RLuc* reported levels of virus replicase increased with time in immature neurons. At 4 and 8 h, mature neurons showed similar levels of virus replicase to immature neurons but thereafter no increase in replicase levels was observed and levels in mature neurons were 20-fold lower than in immature neurons by 16 h (Figure 7a). As expected, given the power of the alphavirus subgenomic promoter, *Rluc*-reported levels of virus structural protein were much higher than those of virus replicase protein; nevertheless, a similar but more rapid shut-off of structural protein synthesis was observed in mature neurons with a >100-fold difference at 16 h (Figure 7b).

Discussion

Relative to SFV4, the delay in replication of SFV4(3H)-eGFP and SFV4-steGFP in the one-step growth curves in BHK-21 cells could be due to the increased time required for replication and transcription of these longer genomes. Alternatively, or in addition, delay in infectious virus production could result from reduced efficiency of polyprotein processing. Immunoblotting of SFV4-steGFP–infected BHK-21 cell lysates showed that although most eGFP was present in the molecular weight band corresponding to free protein, some was present in higher molecular weight products, including an eGFP-2A-p62 fusion protein (Figure 1c). Aberrant processing of the structural polyprotein, presumably due at least in part to failure of cleavage after 2A in a proportion of polyproteins, could have interfered with protein trafficking or virus assembly.

Figure 5 eGFP expression in brains of adult mice infected intracerebrally with SFV4(3H)-eGFP (**a, c, g,** and **i**) or SFV4-steGFP (**b, e, h,** and **j**) and immunostaining (*red*) for CNS cell phenotypes; NeuN for neurons (**a, b, d,** and **f**), CNPase for oligodendrocytes (**g** and **h**), and GFAP for astrocytes (**i** and **j**). In SFV4(3H)-eGFP–infected brains, NeuN-positive cells were generally eGFP-negative (**a**) or, rarely, had low levels of eGFP expression (**c** and **d**, *arrow*). In contrast, in SFV4-steGFP–infected brains, many NeuN-positive cells were eGFP-positive (**b**, *arrows*), including cells with clear neuronal morphology as illustrated by these pyramidal neurons (**e** and **f**, *arrows*) in the hippocampus; eGFP was present in the cytoplasm, nucleus, and neurites. In white matter tracts in both SFV4(3H)-eGFP (**g**) and SFV4-steGFP (**h**) infection, there were many double-labeled oligodendrocytes (*arrows* and *inserts*); the area shown in **g** spans the corpus callosum (cc) and cingulate gyrus (cg). (**i** and **j**) Despite the presence of many astrocytes in the areas of infection, no eGFP expression was observed in these cells; **j** shows eGFP-positive hippocampal pyramidal neurons (*arrow*) with eGFP-positive neurites. The bar in each panel represents 20 μm. This figure is reproduced in colour in *Journal of Neurovirology* online.

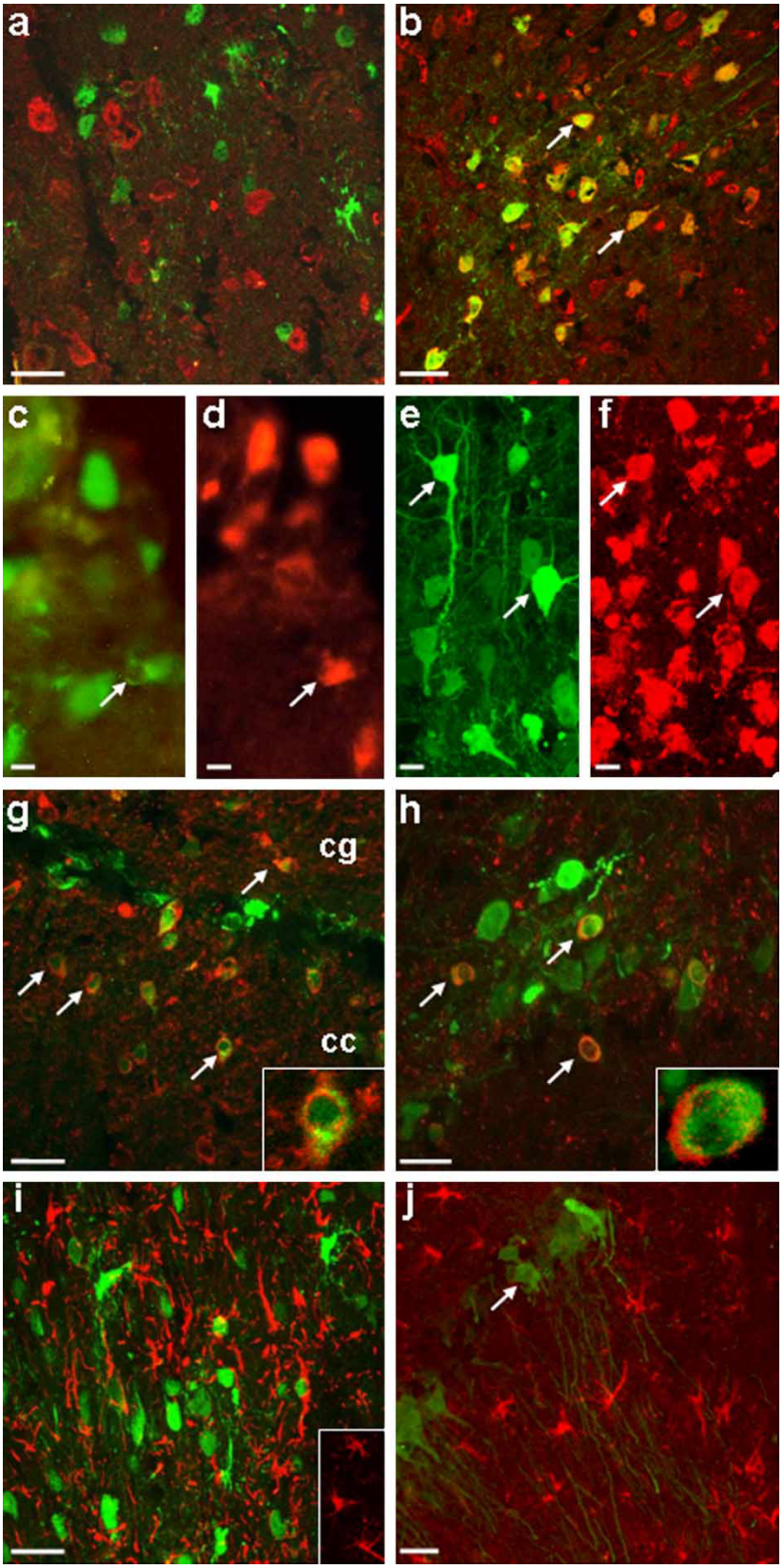

Figure 5 (*Continued*)

Termination of translation after the 2A sequence could also be an issue. Generally, proteins encoded before 2A are found in greater abundance than proteins encoded after 2A (Donnelly *et al*, 2001).

In BHK-21 cells infected with SFV4-steGFP, the eGFP signal was cytoplasmic and mostly perinuclear, whereas in BHK-21 cells infected with SFV4(3H)-eGFP, eGFP was distributed evenly throughout the cytoplasm and the nucleus, a distribution also observed in SFV4-steGFP infected C6/36 cells *in vitro*. Interestingly, BHK-21 cells infected with the very similar SV GFP/2A also exhibit predominantly cytoplasmic fluorescence (Thomas *et al*, 2003), whereas both cytoplasmic and nuclear fluorescence is seen in cells infected with SFV or SV where eGFP is expressed under the control of a duplicated subgenomic promoter (Lundstrom et al, 2003; Frolova et al, 2006; Atasheva et al, 2007). Inefficient 2A cleavage could explain the predominantly perinuclear distribution in this cell type. Widespread eGFP signal observed in other cell types, including C6/36 cells, presumably results from more efficient functioning of the 2A sequence in these cell types.

Previous studies have shown that 10^6 PFU SFV4 inoculated intraperitoneally into adult Balb/c mice kills 60% to 90% (Glasgow et al, 1991; Tarbatt et al, 1997; Tuittila and Hinkkanen, 2003). In the present study, intraperitoneal inoculation of 5000 PFU SFV4- or SFV4-eGFP–expressing viruses resulted in no clinical signs or evidence of brain infection. This same dose of SFV L10 or SFV A7(74) produced high levels of viremia and encephalitis. The inability of SFV4-based viruses to invade the brain can be attributed to the low plasma viraemia. In mice with no type-I interferon response, 5000 PFU SFV4 or SFV4-steGFP produces a high-titer plasma viremia and virus spreads in the brain (Fragkoudis *et al*, 2007). Whereas the ability of SFV4-based viruses to replicate in peripheral tissues and establish neuroinvasion is strongly curtailed by type-I interferon, these viruses replicated well when inoculated directly into the brain. That the eGFP marker viruses infected neurons and oligodendrocytes but not astrocytes is consistent with studies with other strains (Gates et al, 1985; Balluz et al, 1993; Fazakerley et al, 2006). SV also infects neurons, whereas Eastern and Venezuelan equine encephalitis viruses infect neurons, oligodendrocytes, and astrocytes (Schoneboom et al, 1999; Del Piero et al, 2001). As with other marker neurotropic viruses (Ludlow *et al*, 2007), these SFV marker viruses showed strong eGFP and good microscopic resolution of infected cells in brain tissue sections.

As with SFV A7(74) (Fazakerley *et al*, 2006), direct intracerebral inoculation of eGFP marker viruses resulted in widespread infection of white matter tracts. This included many cells with a location and distribution characteristic of oligodendrocytes. Many eGFP-positive cells in white matter tracts, or with a location characteristic of satellite oligodendrocytes, were immunostained with the oligodendrocyte-specific marker CNPase. Infection of oligodendrocytes with SFV4(3H)-eGFP or SFV4-steGFP consistently demonstrated both cytoplasmic and nuclear eGFP localization. As expected, given the higher level of expression from the subgenomic promoter and the rapid degradation of replicase expressed eGFP, eGFP expression was stronger in SFV4-steGFP–infected cells than in SFV4(3H)-eGFP–infected cells. As judged by immunostaining for both nsP3 and structural protein, most oligodendrocytes infected with SFV4(3H)-eGFP expressed eGFP, suggesting ongoing replicase translation in this cell type.

In the mouse brain, both marker viruses infected many neurons and oligodendrocytes. Following infection with SFV4-steGFP, eGFP signal was apparent later than nsP3 and was strong in all infected cells. In contrast, following infection with SFV4(3H)-eGFP, strong eGFP signal was observed only in oligodendrocytes; eGFP signal was very low or absent in nearly all infected neurons. The eGFP derived from SFV4(3H)-eGFP has a very short (<2 h) half-life (Tamberg *et al*, 2007) and thus reports ongoing replicase protein synthesis; its very low level or absence in infected neurons indicates that replicase protein synthesis was rapidly suppressed in neurons. A similar suppression was also seen in SFV4(3H)-eGFP– and SFV4(3H)-*Rluc*–infected primary cultures of mature neurons. The *in vitro* studies demonstrated that mature neurons also rapidly down-regulated structural protein synthesis. It is likely that this also happened *in vivo* but was not observed due to the very high levels of eGFP expressed from the subgenomic promoter (SFV4-steGFP) and the much longer half-life of this eGFP relative to that of eGFP expressed from the genomic promoter (SFV4(3H)-eGFP). These marker viruses provide powerful tools to dissect virus pathogenesis and they clearly distinguish cells at early and late stages of infection in the mouse brain and demonstrate that the course of infection differs between neurons and oligodendrocytes; neurons down-regulate virus replication much faster than oligodendrocytes.

Materials and methods

Construction of SFV4-steGFP

Using site-directed mutagenesis and oligonucleotide duplex insertion, a polylinker containing *Apa* I and *Bam* HI restriction sites followed by the sequence for the foot-and-mouth disease virus (FMDV) 2A peptide were inserted in frame between the regions encoding the capsid and the p62 protein (Figure 1). This construct was designated pSFV4-st and is similar to that described for Sindbis virus (Thomas

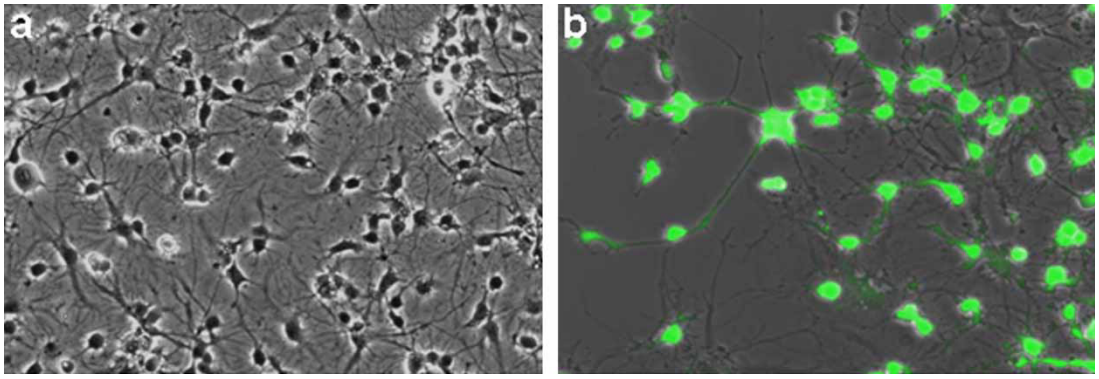

Figure 6 Mature hippocampal neurons infected (MOI 10, 16 h) with SFV4(3H)-eGFP (**a**) or SFV4-steGFP (**b**); phase contrast with eGFP signal. Neurons infected with SFV4(3H)-eGFP had no detectable eGFP at this time point. Neurons infected with SFV4-steGFP had high levels of eGFP in the cytoplasm, neurites and nucleus. This figure is reproduced in colour in *Journal of Neurovirology* online.

et al, 2003). The efficiency of the 2A peptide is affected by amino acids at its N- and C-termini (Ryan *et al*, 1991); the 16 amino acids of 2A were therefore flanked by 3 from the C-terminus of the FMDV 1D protein and proline from the N-terminus of the FMDV 2B protein. Previous studies indicate that the proteolytic activity of the alphavirus capsid protein is independent of downstream sequences (Sjoberg et al, 1994; Frolov et al, 1996). However, to ensure proper processing of the capsid protein from the rest of the structural polyprotein, the first three amino acids of the p62 protein were duplicated between the capsid and the polylinker. The eGFP gene was amplified with primers incorporating *Apa* I and *Bam* HI restriction sites and cloned into pSFV4-st to generate pSFV4-steGFP. pSFV4(3H)-eGFP and pSFV-steGFP were also modified to replace eGFP with the *Renilla* luciferase gene (*RLuc*) to generate pSFV4(3H)-*RLuc* and pSFV4-st*RLuc*. Construction of SFV4(3H)-eGFP (Figure 1) and the short half-life of eGFP expressed in the replicase polyprotein of this virus have been described previously (Tamberg *et al*, 2007).

Viruses

SFV4, SFV4(3H)-eGFP, SFV4-steGFP, SFV4(3H)-*Rluc*, and SFV4-st*RLuc* were generated from their respective icDNAs by electroporation of *in vitro* transcribed RNAs as described previously for SFV4 (Liljestrom *et al*, 1991; Tamberg *et al*, 2007). SFV A7(74) and SFV L10 were derived from natural isolates and have been well-characterized as avirulent and virulent, respectively, in adult mice (Bradish *et al*, 1971; Fazakerley, 2002).

Cell culture studies

BHK-21 cells were used to propagate and titrate viruses as described previously (Fazakerley *et al*, 1993). C6/36 *Aedes albopictus* cells were purchased from the European Collection of Cell Cultures and maintained in L-15 medium (Leibovitz) containing 10% fetal calf serum (FCS), 10% tryptose phosphate broth, and l-glutamine (2 mM) at 28°C without additional CO_2. To passage the cells, medium was removed, the cell monolayer rinsed with fresh L-15 medium, and the cells dislodged with a scraper and resuspended in fresh media in new flasks. Rat hippocampal neurons were isolated from rat pup brains and plated (~150,000 cells/well) onto poly-d-lysine–coated coverslips in 6-well plates. Cells were maintained using neurobasal-A/B-27 growth medium containing 10% horse serum, l-glutamine (0.5 mM), B-27 supplement (1 ml of 50 × per 50 ml), penicillin, and streptomycin (125 U/ml). Plates were maintained in a humidified environment with 5% CO_2. Cells were maintained in culture for 5 or 19 days before infection.

Biochemical analyses

Western blotting on cell lysates of infected BHK-21 cells was carried out as described previously (Tamberg *et al*, 2007). Stability of SFV4-steGFP–expressed eGFP was determined by infection (MOI 10) of BHK-21 cells followed by pulse-chase labeling. At 5 h post infection, cells were washed with phosphate-buffered saline (PBS) and incubated with methionine- and cysteine-free medium for 45 min. Cells were then pulsed for 45 min with methionine- and cysteine-free medium containing 50 μCi S^{35}-labeled methionine and cysteine (Easytag Protein labelling mix; Perkin Elmer). Cells were then washed with PBS and collected or incubated with complete medium containing 10-fold excess of unlabeled methionine and cysteine for 1, 3, or 16 h. eGFP was immunoprecipitated and analyzed as previously described (Lulla et al, 2006; Kiiver et al, 2008).

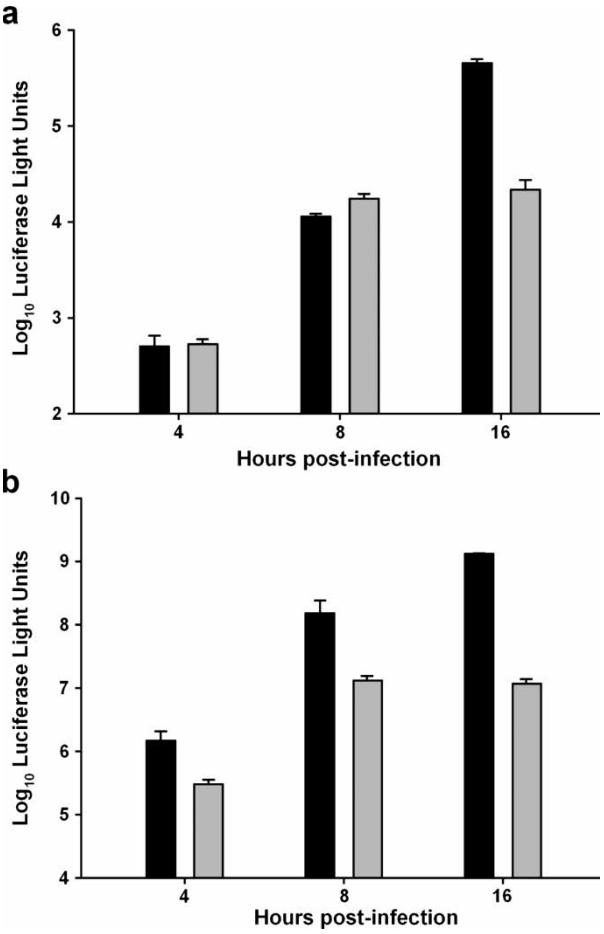

Figure 7 Levels of *RLuc* activity in primary cultures of rat hippocampal neurons at 5 (■) and 19 (■) days post culture following infection with SFV4(3H)-*RLuc* (**a**) and SFV4-st*RLuc* (**b**). Each bar represents the mean of triplicates and the error bars show the standard deviation of these means.

Luciferase assays
Immature (5 days in culture) or more mature (19 days in culture) primary rat hippocampal neuron cultures were infected with SFV4(3H)-*RLuc* or SFV4-st*RLuc* at an MOI of 10 for 4, 8, or 16 h. Cells were lysed in 200 μl Passive Lysis Buffer. *Renilla* luciferase activity was measured using a Dual Luciferase assay kit (Promega) on a GloMax 20/20 Luminometer. To verify the efficiency of infection parallel cultures were immunostained with an anti-nsP3 antibody.

One-step growth curves
In triplicate, BHK-21 monolayers were infected with virus at a multiplicity of infection (MOI) of 10 in Glasgow's Minimal Essential Medium (GMEM) in a humid chamber at room temperature with constant gentle shaking. After 1 h monolayers were washed 3 × with PBSA to remove unbound virus and fresh prewarmed 10% GMEM was added. This was time point 0. Thereafter, every 2 h, 200 μl of virus containing supernatant was collected and replaced with an equal amount of fresh medium.

Assessment of virus genetic stability
Virus phenotypic stability was assessed by passage through BHK-21 cells or mouse brains. After each passage the percentage of plaques giving rise to eGFP-positive cells was determined; 96-plaques were picked and transferred individually into wells of 24-well plates seeded with BHK-21 cells.

Infection of mice
Mice were maintained in the CID animal unit, College of Medicine and Veterinary Medicine, University of Edinburgh, under pathogen-free conditions, with environmental enrichment, a 12-h light/dark cycle and food and water supplied *ad libitum*. All experiments were carried out under the authority of a UK Home Office license. Mice were inoculated with virus in 0.75% PBSA (PBS containing 0.75% of bovine serum albumin [BSA]). Mice were checked twice daily and euthanized at defined times post infection or upon reaching clinically defined terminal end points indicative of terminal disease (Fragkoudis et al, 2007). Mice to be sampled were deeply anesthetized with halothane/O_2 and exsanguinated. Heparinized blood was collected. Brains were removed, bisected sagittally down the midline. Half brains were snap frozen on dry ice for virus titration, submerged immediately in 2 ml RNA*later* to preserve RNA and stored at 4°C or processed for histology.

Histopathology studies
Tissues were immersion fixed for >24 h in 4% neutral-buffered formaldehyde, processed through graded sucrose solutions, embedded in OCT, and stored at -80°C. Tissues were sectioned (12 μm) onto poly-lysine–coated slides. For immunostaining, cryosections were dried and either treated with 0.3% Triton-X100 for 15 min at room temperature or with proteinase K (20 μg/ml) for 15 min at 37°C, followed by a 5-min inactivation step using EDTA/Glycine/PBS. Following membrane permeabilization, slides were washed and treated with CAS block. Primary antibodies were diluted in CAS block and incubated for 2 to 16 h. Slides were then washed and incubated (1 to 3 h) with a biotinylated secondary antibody diluted in CAS block. Sections were washed and streptavidin conjugated Alexa Fluor 594 diluted 1:1400 in H_2O was added (45 min). The slides were then washed and mounted. Sections of uninfected brains and sections of infected brains with no primary or no secondary antibody were used as controls. All washes were 3 × 15 min with PBS. At least three

sections from at least three different, noncontiguous, areas of each brain were examined microscopically.

Declaration of interest: The authors report no conflicts of interest. The authors alone are responsible for the content and writing of the paper.

References

Allsopp TE, Fazakerley JK (2000). Altruistic cell suicide and the specialized case of the virus-infected nervous system. *Trends Neurosci* **23:** 284–290.

Atasheva S, Gorchakov R, English R, Frolov I, Frolova E (2007). Development of Sindbis viruses encoding nsP2/GFP chimeric proteins and their application for studying nsP2 functioning. *J Virol* **81:** 5046–5057.

Atkins GJ, Sheahan BJ, Liljestrom P (1999). The molecular pathogenesis of Semliki Forest virus: a model virus made useful. *J Gen Virol* **80:** 2287–2297.

Balluz IM, Glasgow GM, Killen HM, Mabruk MJ, Sheahan BJ, Atkins GJ (1993). Virulent and avirulent strains of Semliki Forest virus show similar cell tropism for the murine central nervous system but differ in the severity and rate of induction of cytolytic damage. *Neuropathol Appl Neurobiol* **19:** 233–239.

Bradish CJ, Allner K, Maber HB (1971). The virulence of original and derived strains of Semliki Forest virus for mice, guinea-pigs and rabbits. *J Gen Virol* **12:** 141–160.

Del Piero F, Wilkins PA, Dubovi EJ, Biolatti B, Cantile C (2001). Clinical, pathologic, immunohistochemical, and virologic findings of eastern equine encephalomyelitis in two horses. *Vet Pathol* **38:** 451–456.

Donnelly ML, Luke G, Mehrotra A, Li X, Hughes LE, Gani D, Ryan MD (2001). Analysis of the aphthovirus 2A/2B polyprotein 'cleavage' mechanism indicates not a proteolytic reaction, but a novel translational effect: a putative ribosomal 'skip'. *J Gen Virol* **82:** 1013–1025.

Fazakerley JK (2002). Pathogenesis of Semliki Forest virus encephalitis. *J Neuro Virol* **8 (Suppl 2):** 66–74.

Fazakerley JK, Boyd A, Mikkola ML, Kaariainen L (2002). A single amino acid change in the nuclear localization sequence of the nsP2 protein affects the neurovirulence of Semliki Forest virus. *J Virol* **76:** 392–396.

Fazakerley JK, Cotterill CL, Lee G, Graham A (2006). Virus tropism, distribution, persistence and pathology in the corpus callosum of the Semliki Forest virus-infected mouse brain: a novel system to study virus-oligodendrocyte interactions. *Neuropathol Appl Neurobiol* **32:** 397–409.

Fazakerley JK, Pathak S, Scallan M, Amor S, Dyson H (1993). Replication of the A7(74) strain of Semliki Forest virus is restricted in neurons. *Virology* **195:** 627–637.

Fragkoudis R, Breakwell L, McKimmie C, Boyd A, Barry G, Kohl A, Merits A, Fazakerley JK (2007). The type I interferon system protects mice from Semliki Forest virus by preventing widespread virus dissemination in extraneural tissues, but does not mediate the restricted replication of avirulent virus in central nervous system neurons. *J Gen Virol* **88:** 3373–3384.

Frolov I, Hoffman TA, Pragai BM, Dryga SA, Huang HV, Schlesinger S, Rice CM (1996). Alphavirus-based expression vectors: strategies and applications. *Proc Natl Acad Sci U S A* **93:** 11371–11377.

Frolova E, Gorchakov R, Garmashova N, Atasheva S, Vergara LA, Frolov I (2006). Formation of nsP3-specific protein complexes during Sindbis virus replication. *J Virol* **80:** 4122–4134.

Gates MC, Sheahan BJ, O'Sullivan MA, Atkins GJ (1985). The pathogenicity of the A7, M9 and L10 strains of Semliki Forest virus for weanling mice and primary mouse brain cell cultures. *J Gen Virol* **66(Pt 11):** 2365–2373.

Glasgow GM, Sheahan BJ, Atkins GJ, Wahlberg JM, Salminen A, Liljestrom P (1991). Two mutations in the envelope glycoprotein E2 of Semliki Forest virus affecting the maturation and entry patterns of the virus alter pathogenicity for mice. *Virology* **185:** 741–748.

Griffin DE (2005). Neuronal cell death in alphavirus encephalomyelitis. *Curr Top Microbiol Immunol* **289:** 57–77.

Kiiver K, Tagen I, Zusinaite E, Tamberg N, Fazakerley JK, Merits A (2008). Properties of non-structural protein 1 of Semliki Forest virus and its interference with virus replication. *J Gen Virol* **89:** 1457–1466.

Kujala P, Ikaheimonen A, Ehsani N, Vihinen H, Auvinen P, Kaariainen L (2001). Biogenesis of the Semliki Forest virus RNA replication complex. *J Virol* **75:** 3873–3884.

Lemm JA, Rice CM (1993). Assembly of functional Sindbis virus RNA replication complexes: requirement for coexpression of P123 and P34. *J Virol* **67:** 1905–1915.

Liebert UG, Baczko K, Budka H, ter Meulen V (1986). Restricted expression of measles virus proteins in brains from cases of subacute sclerosing panencephalitis. *J Gen Virol* **67:** 2435–2444.

Liebert, UG, Schneider-Schaulies, S, Baczko, K, ter, M, V (1990). Antibody-induced restriction of viral gene expression in measles encephalitis in rats. *J Virol* **64**, 706–713.

Liljestrom P, Lusa S, Huylebroeck D, Garoff H (1991). In vitro mutagenesis of a full-length cDNA clone of Semliki Forest virus: the small 6,000-molecular-weight membrane protein modulates virus release. *J Virol* **65:** 4107–4113.

Ludlow M, Duprex WP, Cosby SL, Allen IV, McQuaid S (2008). Advantages of using recombinant measles viruses expressing a fluorescent reporter gene with vibratome slice technology in experimental measles neuropathogenesis. *Neuropathol Appl Neurobiol* **34**:424–434

Lulla V, Merits A, Sarin P, Kaariainen L, Keranen S, Ahola T (2006). Identification of mutations causing temperature-sensitive defects in Semliki Forest virus RNA synthesis. *J Virol* **80:** 3108–3111.

Lundstrom K, Abenavoli A, Malgaroli A, Ehrengruber MU (2003). Novel Semliki Forest virus vectors with reduced cytotoxicity and temperature sensitivity for long-term enhancement of transgene expression. *Mol Ther* **7:** 202–209.

Oldstone MB, Buchmeier MJ (1982). Restricted expression of viral glycoprotein in cells of persistently infected mice. *Nature* **300:** 360–362.

Oliver KR, Scallan MF, Dyson H, Fazakerley JK (1997). Susceptibility to a neurotropic virus and its changing distribution in the developing brain is a function of CNS maturity. *J Neuro Virol* **3:** 38–48.

Pathak S, Webb HE (1983). Semliki Forest virus multiplication in oligodendrocytes in mouse- brain with reference to demyelination. *J Physiol* (Lond), 339, 17.

Pusztai R, Gould E, Smith H (1971). Infection pattern in mice of an avirulent and virulent strain of Semliki Forest virus. *Br J Exp Pathol* **52:** 669–677.

Ryan MD, King AM, Thomas GP (1991). Cleavage of foot-and-mouth disease virus polyprotein is mediated by residues located within a 19 amino acid sequence. *J Gen Virol* **72(Pt 11):** 2727–2732.

Salonen A, Vasiljeva L, Merits A, Magden J, Jokitalo E, Kaariainen L (2003). Properly folded nonstructural polyprotein directs the semliki forest virus replication complex to the endosomal compartment. *J Virol* **77:** 1691–1702.

Scallan MF, Fazakerley JK (1999). Aurothiolates enhance the replication of Semliki Forest virus in the CNS and the exocrine pancreas. *J NeuroVirol* **5:** 392–400.

Schoneboom BA, Fultz MJ, Miller TH, McKinney LC, Grieder FB (1999). Astrocytes as targets for Venezuelan equine encephalitis virus infection. *J NeuroVirol* **5:** 342–354.

Sjoberg EM, Suomalainen M, Garoff H (1994). A significantly improved Semliki Forest virus expression system based on translation enhancer segments from the viral capsid gene. *Bio-Technology* **12:** 1127–1131.

Strauss JH, Strauss EG (1994). The alphaviruses: gene expression, replication, and evolution. *Microbiol Rev* **58:** 491–562.

Tamberg N, Lulla V, Fragkoudis R, Lulla A, Fazakerley JK, Merits A (2007). Insertion of EGFP into the replicase gene of Semliki Forest virus results in a novel, genetically stable marker virus. *J Gen Virol* **88:** 1225–1230.

Tarbatt CJ, Glasgow GM, Mooney DA, Sheahan BJ, Atkins GJ (1997). Sequence analysis of the avirulent, demyelinating A7 strain of Semliki Forest virus. *J Gen Virol* **78:** 1551–1557.

Thomas JM, Klimstra WB, Ryman KD, Heidner HW (2003). Sindbis virus vectors designed to express a foreign protein as a cleavable component of the viral structural polyprotein. *J Virol* **77:** 5598–5606.

Tuittila M, Hinkkanen AE (2003). Amino acid mutations in the replicase protein nsP3 of Semliki Forest virus cumulatively affect neurovirulence. *J Gen Virol* **84:** 1525–1533.

This paper was first published online on iFirst on 24 December 2008.